

# MOD 201: The Neuron and its Dynamics

Ciprian Bangu

March 22 2024

## Contents

<b>1</b>	<b>Introduction</b>	<b>2</b>
<b>2</b>	<b>Modelling Spike Trains</b>	<b>2</b>
2.1	A single spike train . . . . .	2
2.2	Multiple spike trains, multiple trials . . . . .	3
2.3	The interspike interval . . . . .	4
<b>3</b>	<b>Analyzing Spike Trains</b>	<b>4</b>
3.1	The somatosensory neuron . . . . .	5
3.2	Different stimulus intensities . . . . .	6
3.3	Summary . . . . .	8
<b>4</b>	<b>Models of the neuron</b>	<b>8</b>
4.1	The integrate-and-fire model . . . . .	8
4.1.1	The current dynamics . . . . .	8
4.1.2	The spiking mechanism . . . . .	11
4.1.3	Noisy Integrate and Fire . . . . .	12
4.1.4	Time varying current . . . . .	13
4.2	The Hodgkin-Huxley model . . . . .	13
4.2.1	Voltage gated ion channels . . . . .	14
4.2.2	Simulating the H & H model . . . . .	14
4.2.3	H & H model with varying injected current . . . . .	16
4.2.4	Summary . . . . .	16
<b>5</b>	<b>Conclusion</b>	<b>16</b>

# 1 Introduction

Neurons are a fundamental aspect of the brain. They are responsible for processing and transmitting information throughout the brain. In this report, we will model their behavior at the macro level, looking at spike trains, and then compare these models to real data. We will then explore the dynamics of individual neurons by looking at two models of the neuron: the Integrate and Fire model, and the Hodgkin-Huxley model.

## 2 Modelling Spike Trains

When presented with a stimulus it is sensitive to, a neuron will fire a series of action potentials, or 'spikes'. This series of spikes is called a *spike train*.

Real neurons are biological entities, and are thus noisy in their behavior. This means that, even given the same stimulus and average firing rate, a neuron will not produce the same spike train every time. Rather, the behavior is probabilistic; that a neuron will fire at each time step is given by a probability function. Specifically, neuronal firing behavior can be modeled by the Poisson distribution:

$$P_n(T) = (rT)^n \frac{e^{-rT}}{n!} \quad (1)$$

Where  $P_n(T)$  is the probability of observing  $n$  spikes in a time window of length  $T$ , and  $r$  is the average firing rate of the neuron.

### 2.1 A single spike train

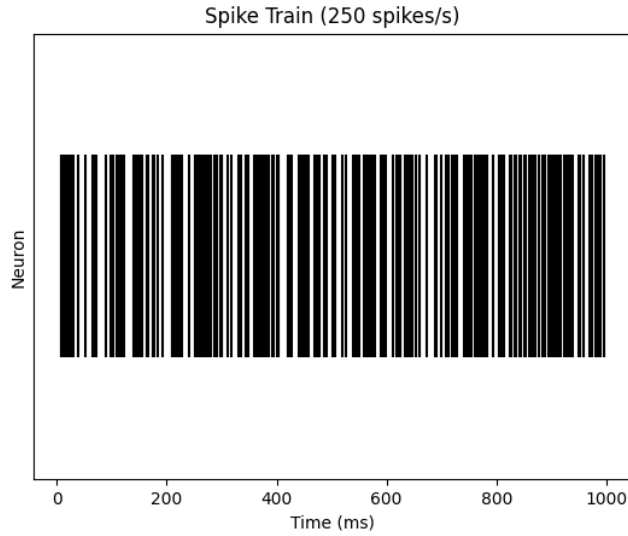


Figure 1: Raster plot for simulated spike train for a single neuron on a single trial.  $r = 250\text{hz}$ .

Figure 1 is a raster plot, showing a simulated spike train for a single neuron on a single trial. The x-axis represents time in milliseconds, and each line in the plot represents a spike. This neuron has an average firing rate of 250hz, or 250 spikes per second.

## 2.2 Multiple spike trains, multiple trials

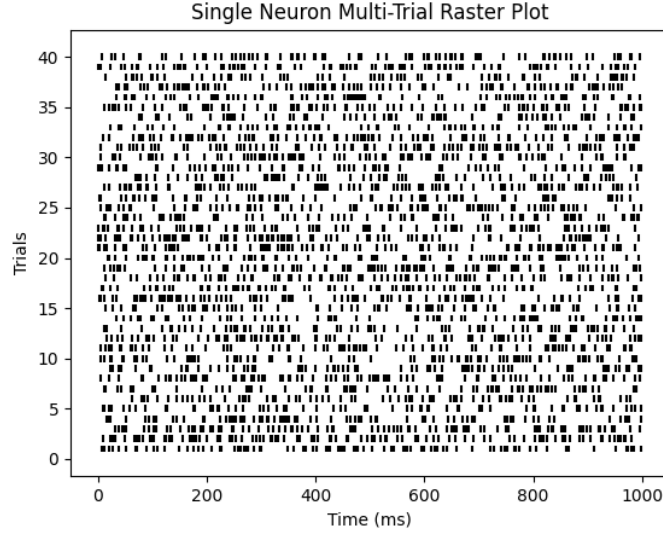


Figure 2: A raster plot of 40 simulated spike trains, where the  $r = 80\text{hz}$ .

The variability in firing behavior is better seen in figure 2, which shows a raster plot of 40 simulated spike train trials, where the average firing rate of the neuron is 80hz. Although the parameters of the neuron are the same for each trial, the spike trains are different, owing to the probabilistic behavior of the neuron.

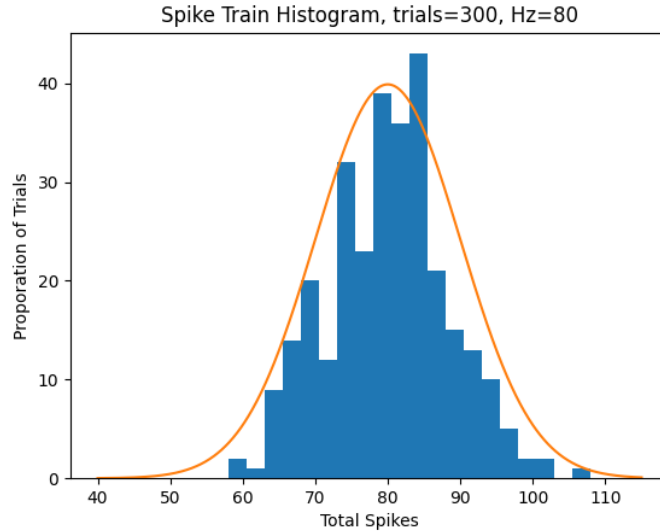


Figure 3: Histogram of spike counts for 300 simulated spike trains, where  $r = 80\text{hz}$ . The orange curve represents the normal distribution with  $\mu = 80$  and  $\sigma = 10$

Figure 3 shows a histogram of spike counts for 300 simulated spike trains, where the firing rate of the neuron is 80hz. This allows us to visualize the variability in spike counts across trials. While the average is 80 spikes, we see that the number (in this simulation) goes as low as 50, and as high as 109. Additionally, we can see that the distribution of spike counts is approximately normal. This is evidenced by the orange curve, which represents the normal distribution with a mean of 80, and a standard deviation of 10. This behavior is to be expected, as the Poisson distribution approximates the normal distribution for large values of  $rT$ , i.e., for large values of the average spike count.

### 2.3 The interspike interval

As we have seen in Figs. 1 and 2, neurons do not fire continuously throughout the trial period. Rather, their activity is spread out over time. The time interval between spikes is the known as the *interspike interval*. Given that the probability of a spike is given by the Poisson distribution, we should predict that the interspike intervals are exponentially distributed.

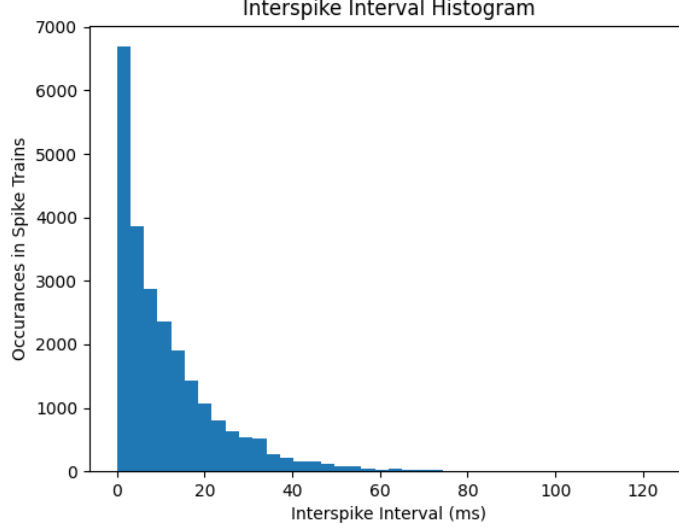


Figure 4: The interspike interval histogram for the same neuron, over 300 trials, where  $r = 80\text{hz}$ .

This relationship is confirmed in Figure 4, which plots the number of occurrences of each interspike interval length for our neuron over the trials. As predicted, the distribution of trials is exponential, with the majority of interspike intervals being short, and the number of long intervals decreasing exponentially.

Moreover, we can compute the coefficient of variance, i.e., standard deviation divided by the mean, for the interspike intervals:

$$CV = \frac{\sigma}{\mu} \quad (2)$$

For a Poisson process, the coefficient of variance is 1. For our neuron, the coefficient of variance is 1.03, which is very close to 1. Given that this simulation was not very large, we can assume that this small discrepancy is due to noise. Thus, the  $CV$  confirms that the interspike intervals were produced by a Poisson Process.

## 3 Analyzing Spike Trains

We can now move from simulated neurons, to recordings of the real thing. In the following section, we will be analyzing data from a real neuron located in the primary somatosensory cortex of a monkey. This neuron was recorded while the monkey was presented with a vibrotactile stimulus on its fingertip. Since the neuron is located in the primary somatosensory cortex, i.e., the part of the brain responsible for processing sensory perception, we might expect it to respond to this stimulus and thus produce spike trains.

### 3.1 The somatosensory neuron

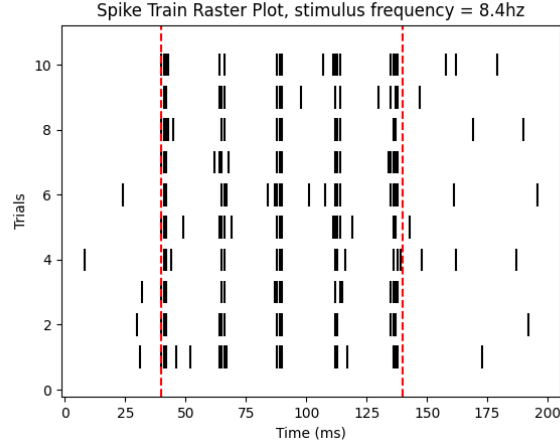


Figure 5: A raster plot of the spike train of the somatosensory neuron, over 10 trials, where the stimulus frequency is 8.4hz. The red horizontal lines represent the onset and offset of the stimulus.

Fig. 5 shows the spike trains generated by the neuron over 10 trials, where the stimulus is a vibration of 8.4hz. As we can see from Fig. 5, the neuron is actually active throughout the recording period. However, it is the most active during the stimulus period. This is demonstrated by the fact that the amount of spikes in the stimulus period, i.e., between the dashed red lines, is far greater than the amount of spikes outside of the stimulus period. This suggests that the neuron is responding to the stimulus.

Table 1: Spike counts in each trial during the stimulus period; stimulus = 8.4hz

Trial 1	Trial 2	Trial 3	Trial 4	Trial 5	Trial 6	Trial 7	Trial 8	Trial 9	Trial 10
18	14	16	14	18	19	18	15	15	18

Table 2: Spike statistics over all trials, during the stimulus period; stimulus = 8.4hz

Mean	Variance	Mean Firing Rate
16.5	3.25	33.0 spikes/s

Tables 1 and 2 summarize the spiking behavior of the neuron during the stimulus period, for the 8.4hz stimulus. From the data we can see that, like our model, the neuron does not fire the same amount of spikes in each trial. On average, over the trials the neuron spikes 16.5 times during the stimulus period, with a variance of 3.25. This gives us a mean firing rate of 33.0 spikes/s for this neuron when presented with this stimulus.

We can also measure the density of the spikes in each time-bin. The spike density is given by the following equation:

$$p = \frac{1}{\Delta t} \frac{n_K(t; t + \Delta t)}{K} \quad (3)$$

where  $\Delta t$  is the time step,  $n_K(t; t + \Delta t)$  is the number of spikes in the time window, and  $K$  is the number of trials. The spike density plot is shown in Figure 6. For this experiment, the data uses a time step of 5ms. From the plot, we can see that for this stimulus, the neuron is active in bursts: the vast majority of the spikes happen in 5 time bins. This is consistent with the behavior observed in Figure 5., where we saw a similar grouping of spikes. Moreover, the stimulus does not elicit a very strong response from the neuron: the highest density of spikes is only 0.2 spikes/5ms.

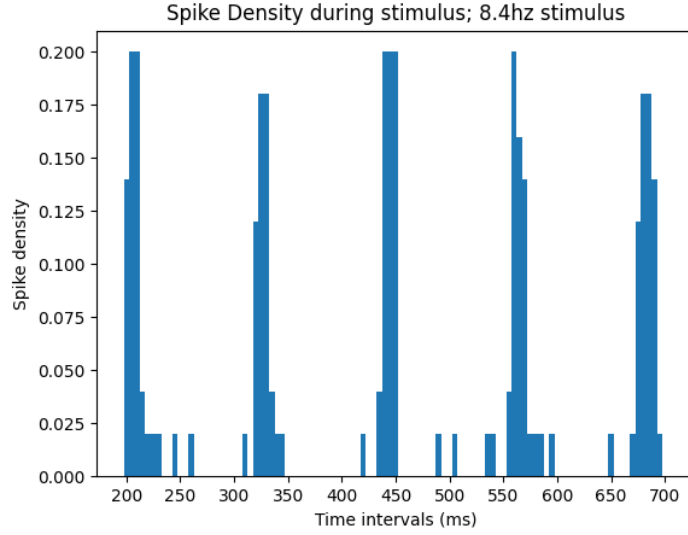


Figure 6: Spike density bar plot for the somatosensory neuron during the stimulus period, over 10 trials, where the stimulus frequency is 8.4hz.  $\Delta t = 5(ms)$

### 3.2 Different stimulus intensities

We have seen that the neuron does respond to the stimulus, however not very strongly. Let us now investigate what happens when we increase the intensity of the stimulus, i.e., increase the frequency of the vibration. Again, to investigate the behavior of the neuron, we can visualize its generated spike trains in a raster plot. Figure 7, below, shows the raster plot of the neuron's response to all of the stimuli in the experiment. As we can see from Fig. 7, as the stimulus intensity increases, the neuron's response becomes stronger. This is evidenced by the increase in the number of spike trains produced by the neuron during the stimulus period. At 8.4hz, the neuron only produces 5 spike trains; at 35hz, the neuron produces 18 spike trains.

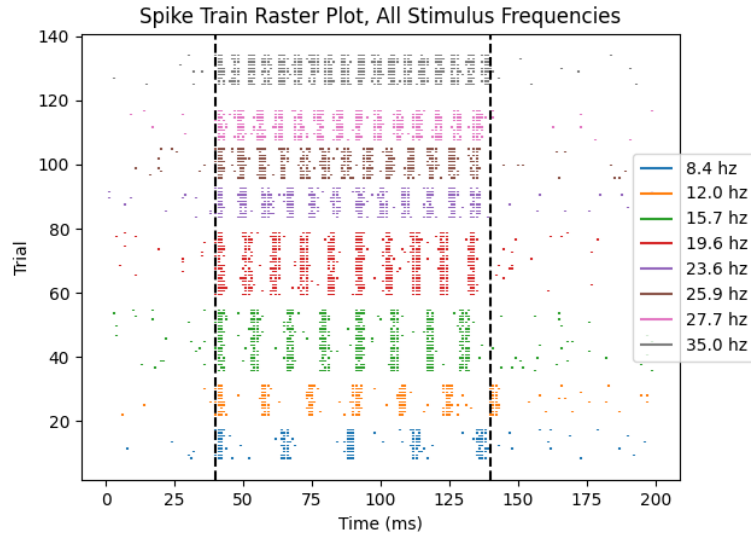


Figure 7: A raster plot showing the neurons response to every stimulus frequency presented, over varying numbers of trials. Stimulus onset and offset denoted by black dashed lines.

The density of the spike trains has also changed. This can be observed in the spike density plots, shown in Fig. 8. Not only does the maximum density increase as the the stimulus intensifies, but the minimum density also increases. This suggests that the neuron is more active in general.

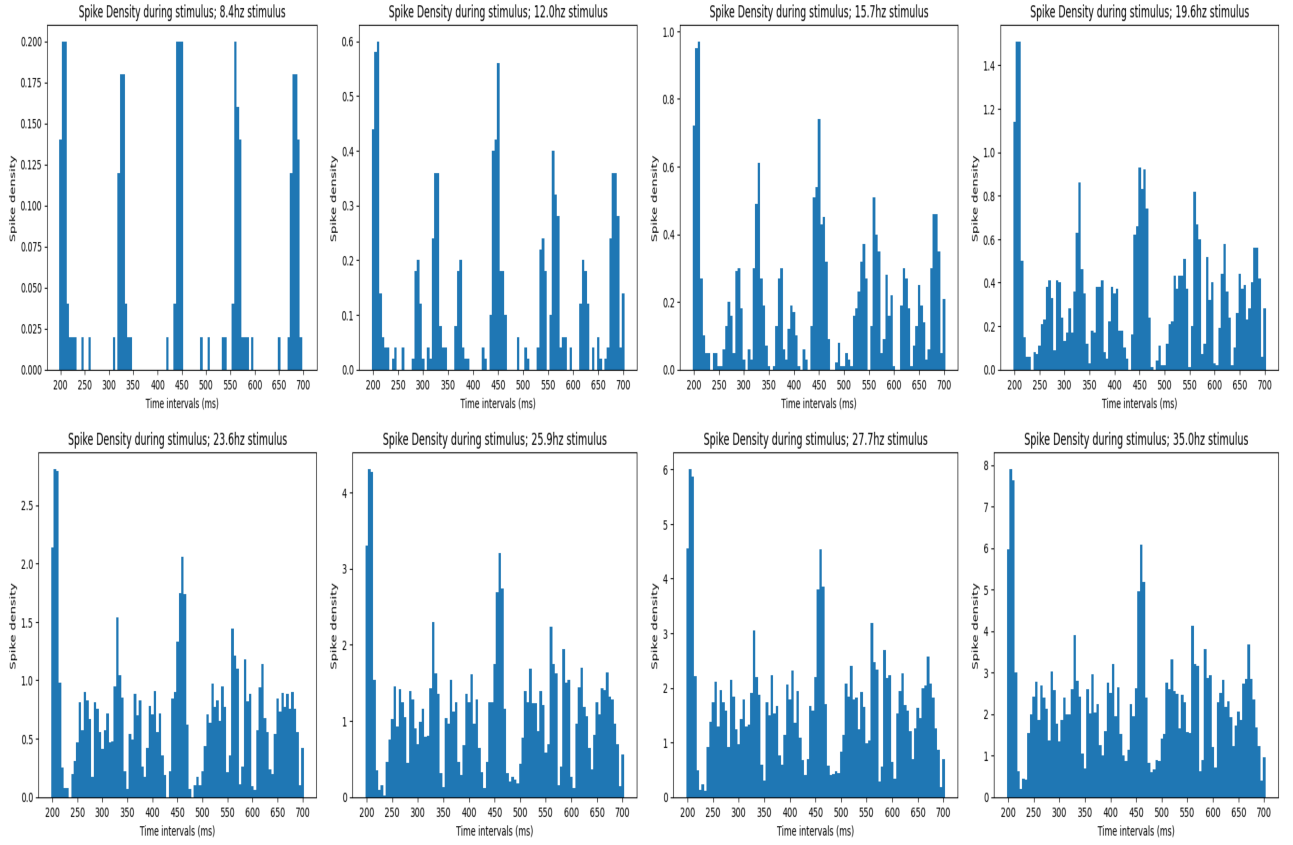


Figure 8: Spike density bar plots for all stimulus frequencies. Between 10 and 20 trials for each stimulus,  $\Delta t = 5(ms)$

Table 3 details the spike count statistics over all the trials for each stimulus. As we can see, the mean number of spikes increases as the stimulus frequency increases. This confirms the observations made from Figs. 7 and 8. Moreover, the mean firing rate of the neuron also increases as the stimulus frequency increases. It begins at 33.0 spikes/s for the 8.4hz stimulus, and ends at 105.8 spikes/s for the 35hz stimulus.

Table 3: Spike count statistics over all trials, during the stimulus period; varying stimulus frequencies

Stimulus Frequency	Mean	Variance	Mean Firing Rate
8.45 hz	16.5	3.25	33.0 spikes/s
12.0 hz	19.9	2.09	39.8 spikes/s
15.7 hz	23.6	3.84	47.2 spikes/s
19.6 hz	29.9	2.489	59.8 spikes/s
23.6 hz	35.6	6.239	71.2 spikes/s
25.9 hz	39.5	8.65	79.0 spikes/s
27.7 hz	41.8	3.559	83.6 spikes/s
35.0 hz	52.9	11.09	105.8 spikes/s

Figure 9 is the tuning curve for this neuron and stimulus, and allows us to visualize this increase in mean firing rate for the neuron. From Fig. 9 we can see that there is positive (nearly) linear relationship between an increase in stimulus intensity, and the mean firing rate of the neuron.

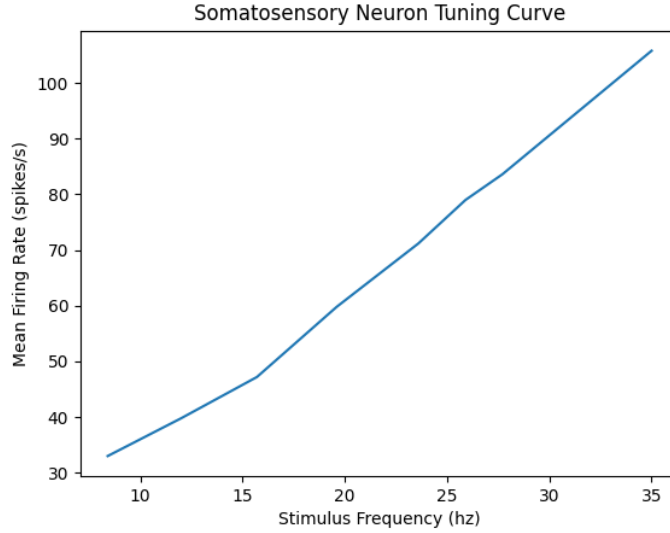


Figure 9: The tuning curve of the somatosensory neuron.

### 3.3 Summary

In this section, we have simulated the behavior of a neuron at the level of the spike train, and analyzed real spike train data from a monkey somatosensory neuron. We have seen that neuronal spike trains are probabilistic and noisy. We have also seen that neurons increase their spike train production in response to a stimulus they are tuned to, and more intense stimuli lead to a greater response. In the next section, we will move from the level of the spike train to the level of the individual neuron, and explore models of how neurons generate the spikes we have analyzed in this section.

## 4 Models of the neuron

In the two previous sections, we have modelled and analyzed the outputs of neuronal function. That is, we have modeled their spiking behavior over time, and we have analyzed their responses to different stimuli. In this section, we will explore models of how neurons generate the spikes that we analyzed in the previous sections.

### 4.1 The integrate-and-fire model

#### 4.1.1 The current dynamics

Neurons, to a first approximation, can be thought of as R-C circuits. Neurons contain, and are surrounded by, ions of different types and charges. At rest, there are more negatively charged ions within the cell than outside, and more positively charged ions outside the cell than inside. This dynamic results in a potential difference across the cell membrane, known as the (resting) membrane potential. In a real neuron, this potential is determined by different ions. However, in the integrate and fire model, the specific effects of different ions are enveloped by the 'leak potential', i.e., determined only by ions that pass through always-open 'leak' channels. Throughout the functioning of the neuron, these ions move in and out of the cell. This movement is in-part mediated by the cell membrane. Thus, the cell membrane acts as a capacitor, in that it separates charges in and outside the cell, and as a resistor, restricting how much the injection of external current changes the membrane potential. Moreover, cell membrane also has a specific conductance, which determines the permeability of the membrane to ions.

This leads us to the simplest model of a neuron: the Integrate and Fire model. It is described by the following Ordinary Differential Equation:

$$C \frac{dV(t)}{dt} = g_L(E_L - V(t)) + I \quad (4)$$

Where  $C$  is the membrane capacitance,  $g_L$  is the membrane conductance,  $E_L$  is the equilibrium (leak) potential,  $I$  is the injected current, and  $V(t)$  is the function of membrane potential over time. For this simulation, we will set  $C = 1$ ,  $g_L = 0.1$ ,  $E_L = -70$ , and  $I = 1$ .

Equation 4 can be solved numerically using Euler's method:



$$\begin{aligned}
V(t + \Delta t) &= V(t) + \frac{dV(t)}{dt} \Delta t \\
V(t + \Delta t) &= V(t) + \frac{1}{C}(g_L(E_L - V(t)) + I)\Delta t
\end{aligned} \tag{5}$$

Figure 10 shows a simulation of the membrane potential over time for an Integrate and Fire neuron, resulting from the implementation of Euler's method. From the figure, we can see that the membrane potential increases over time, to a certain limit (around  $-60mv$ ).

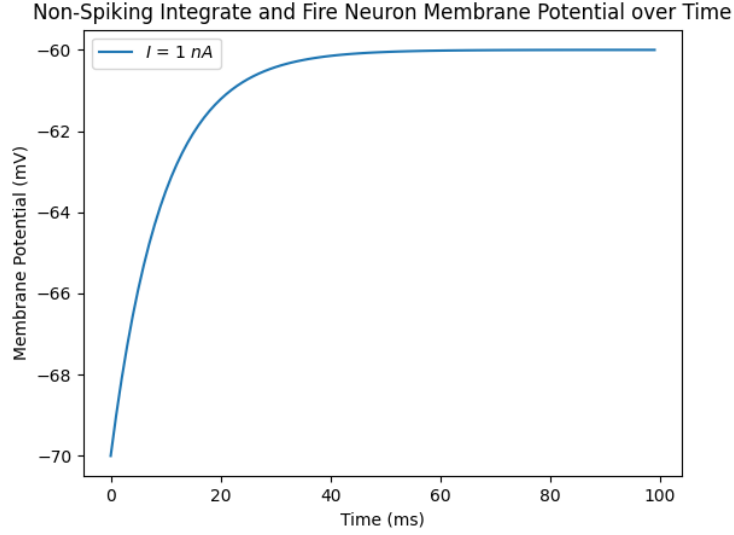


Figure 10: Integrate-and-fire model of a neuron. The injected current  $I = 1nA$ , the resting membrane potential,  $E_L$  is initialized at  $-70mV$ , the conductance is  $g_L = 0.1\mu S$ , and the timestep  $\Delta t = 1ms$

This behavior is to be expected because the analytical solution to the ODE includes an exponentially decaying function, which will asymptotically approach some limit determined by the resting potential and the injected current. Namely:

$$\begin{aligned}
C \frac{dV(t)}{dt} &= g_L(E_L - V(t)) + I \\
\frac{dV}{dt} &= \frac{g_L(E_L - V(t)) + I}{C} && \text{separating variables} \\
\frac{dV}{g_L(E_L - V) + I} &= \frac{dt}{C} && \text{separating } V \text{ and } t \\
\int \frac{dV}{g_L(E_L - V) + I} &= \int \frac{dt}{C} && \text{integrating both sides}
\end{aligned}$$

Substituting  $u = g_L(E_L - V) + I$  and  $du = -g_L dV$ :

$$\begin{aligned}
\int \frac{-1}{g_L} \frac{du}{u} &= \int \frac{dt}{C} \\
-\frac{1}{g_L} \ln |u| &= \frac{t}{C} + K \\
-\frac{1}{g_L} \ln |g_L(E_L - V) + I| &= \frac{t}{C} + K && \text{substituting back } u \\
\ln |g_L(E_L - V) + I| &= -g_L \left( \frac{t}{C} + K \right) && \text{multiplying by } -g_L \\
g_L(E_L - V) + I &= e^{-g_L(\frac{t}{C} + K)} && \text{exponentiating both sides}
\end{aligned}$$

Since we are dealing with a neuron, we know that the membrane potential will remain below 0, so we can ignore the positive case for the absolute value. Thus:

$$\begin{aligned}
g_L(E_L - V) + I &= e^{-g_L(\frac{t}{C} + K)} \\
E_L - V &= \frac{e^{-g_L(\frac{t}{C} + K)} - I}{g_L} \\
V &= E_L - \frac{e^{-g_L(\frac{t}{C} + K)} - I}{g_L}
\end{aligned} \tag{6}$$

Equation 6 is the analytical solution to the ODE, and allows us to compare the numerical and analytical solutions. To fully solve the equation for some initial conditions we need to solve for the constant  $K$ . We can do this by using the initial condition of the neuron. For example, at  $t = 0$ :  $E_L = -70$ ,  $g_L = 0.1$ ,  $C = 1$ ,  $I = 1$ . Thus:

$$\begin{aligned}
-\frac{1}{g_L} \ln |g_L(E_L - V) + I| &= \frac{t}{C} + K \\
-\frac{1}{0.1} \ln |0.1(-70 - (-70)) + 1| &= \frac{0}{1} + K && \text{using initial conditions} \\
-10 \ln |1| &= K \\
K &= 0
\end{aligned}$$

Substituting  $K$  back into the equation, we get:

$$V(t) = -70 - \frac{e^{-0.1(\frac{t}{1} + 0)} - 1}{0.1}$$

Thus we confirm that  $V(0) = -70$  and  $V(100) = -60$  for both the numerical and analytical solutions in both cases.

However, the analytical solution allows us to predict the maximum potential reached by the neuron, given the injected current. For example, if we were to inject a current of  $I = 4nA$ , the maximum potential reached by the neuron would be about  $-30mV$ :

$$V(100) = -70 - \frac{e^{-0.1(\frac{100}{1} + (-10 \ln |4|))} - 4}{0.1} \approx -30$$

This prediction is confirmed by the numerical solution, as shown in Figure 11.

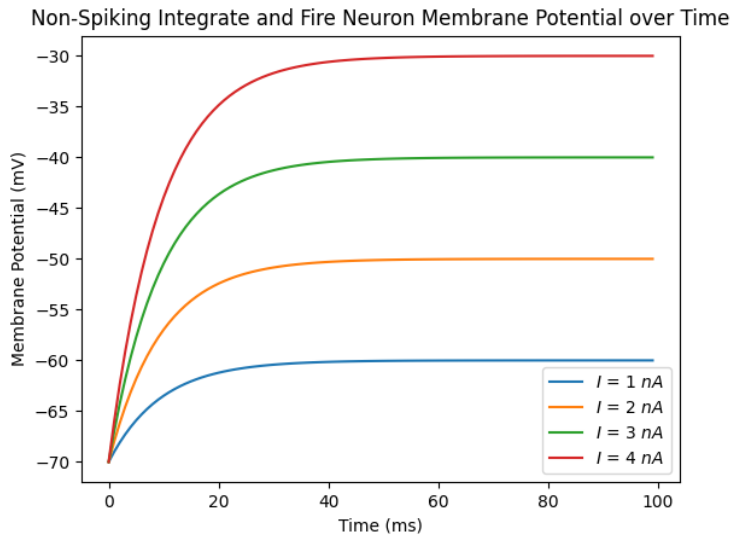


Figure 11: Integrate-and-fire model of a neuron, with varying injected currents. The resting membrane potential,  $E_L$  is initialized at  $-70mV$ , the conductance is  $g_L = 0.1\mu S$ , and the timestep  $\Delta t = 1ms$

Moreover, Fig. 11 illustrates the impact that different injected currents have on the neuron's behavior. Namely, as the injected current increases, the membrane potential has a higher limit.

#### 4.1.2 The spiking mechanism

While Equation 4 models the neuronal dynamic with respect to the current provided, it misses a crucial aspect of neuronal activity, namely the spiking behavior. Biologically, this spiking behavior corresponds to a rapid depolarization of the membrane potential, followed by a rapid repolarization. As we have seen from Figures 10 and 11, the model leads to an increase in membrane potential, but this increase is gradual and asymptotic - once it reaches the maximum it stays there.

In order to make this model more accurately capture the behavior of neurons, we need to add a spiking mechanism. We can do this by adding a membrane potential threshold to the model. This parameter,  $V_{th}$  is value of the potential at which the neuron will fire - i.e., rapidly depolarize. It will continue to rapidly depolarize until it reaches a maximum potential,  $V_{max}$ , after which it will rapidly re-polarize. Figure 12 below, demonstrates this behavior by implementing the model with these additional parameters.

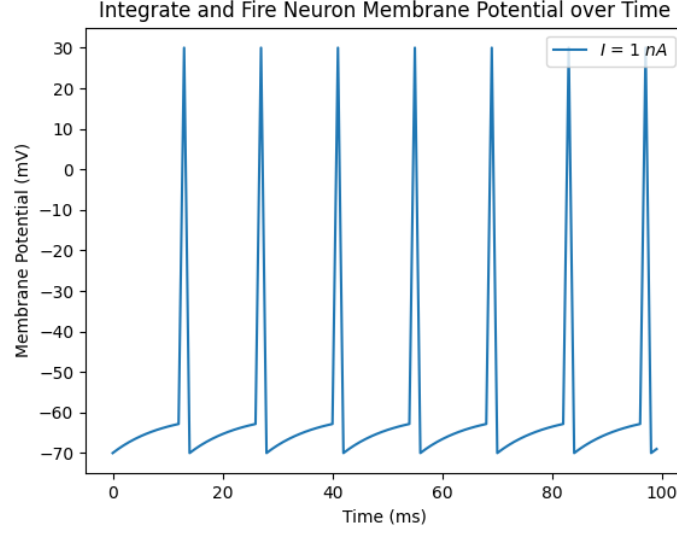


Figure 12: Integrate and fire neuron with spiking behavior. The injected current  $I = 1nA$ , the resting membrane potential,  $E_L$  is initialized at  $-70mV$ , the conductance is  $g_L = 0.1\mu S$ , the threshold  $V_{th} = -63mV$ , the maximum potential  $= V_{max} = 30mV$  and the timestep  $\Delta t = 1ms$

From Fig. 12, we see that when  $I = 1nA$  the neuron fires 7 times in 100ms. In Fig. 13, we see how the number of spikes changes as the injected current changes.

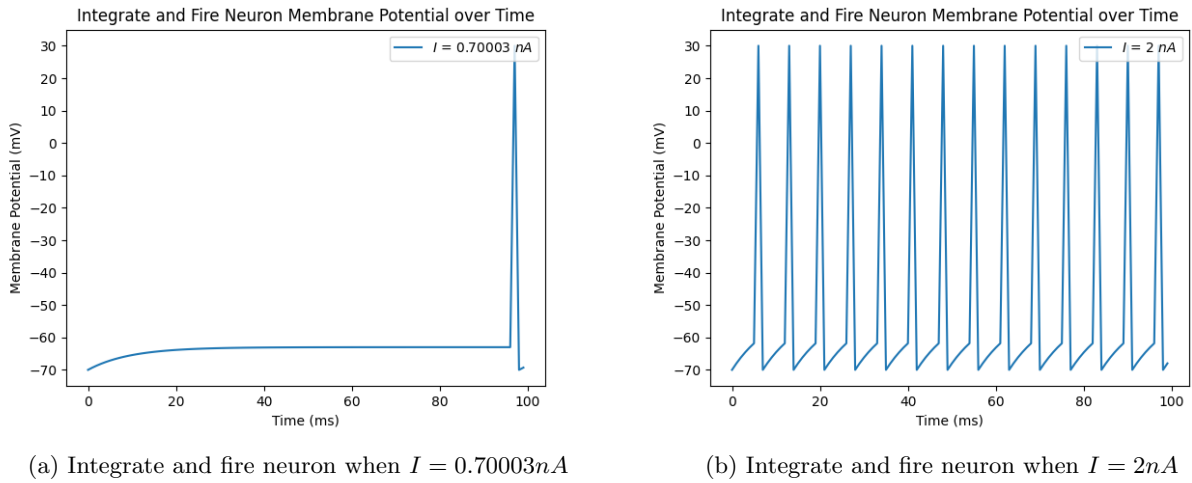


Figure 13: Integrate and fire neuron behavior with varying injected currents.

Fig. 13 demonstrates that the neuron begins to fire when the injected current surpasses  $0.7nA$  - around  $0.70003nA$ . As the current increases, the neuron fires more frequently. Comparing Figures 12 and 13, we see that the neuron fires 7 times in 100ms when  $I = 1nA$ , and 14 times when the current is doubled to  $I = 2nA$ . Fig. 14 below shows the tuning curve of this neuron.

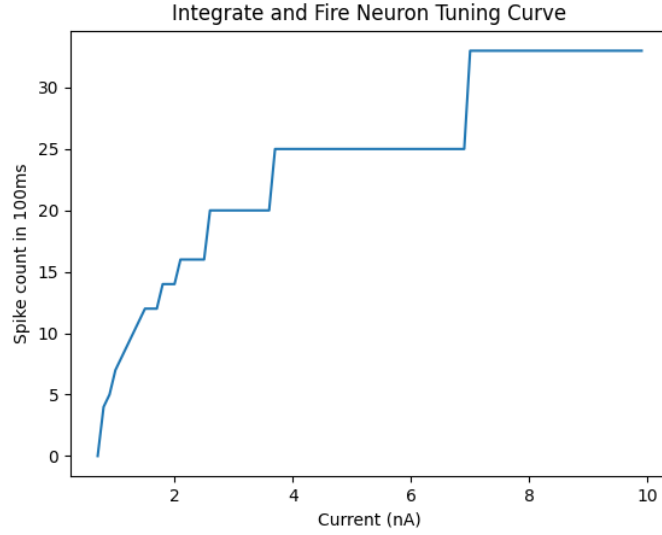


Figure 14: The tuning curve for the integrate and fire neuron, plotting the amount of spikes within 100ms, for varying injected currents.

From Fig. 14, We see that the number of spikes increases linearly in the beginning, and then begins to taper off. Around  $2nA$  it begins to exhibit a plateauing behavior, where the number of spikes the neuron is able to produce within the time window remains constant for increasing currents, until the injected current reaches a threshold at which it stimulates the neuron intensely enough to cause a large increase in the number of spikes. While the amount of current needed to break the plateau increases over time, when it *is* broken, the increase in spikes during the interval is larger than the previous increase.

#### 4.1.3 Noisy Integrate and Fire

As we saw in previous sections, neuronal behavior is noisy. Thus, to accurately model it, we need to add white noise to the model. We can do this by adding a normally distributed random variable to the injected current,  $\eta(t)$ , scaled by a noise factor  $\sigma$ . The updated model is the following:

$$C \frac{dV(t)}{dt} = g_L(E_L - V(t)) + I + \sigma\eta(t) \quad (7)$$

Fig. 15 implements the model in Equation 7, and shows how the behavior of the neuron changes given different noise factors.

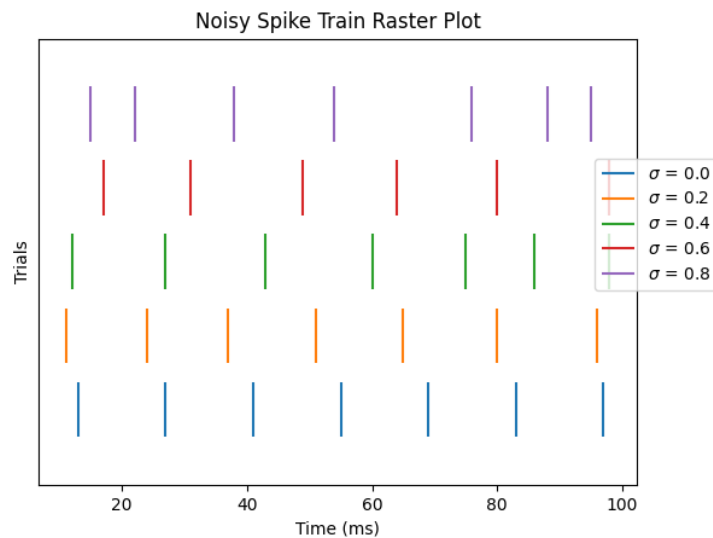


Figure 15: Raster plot for a noisy integrate and fire neuron, with varying  $\sigma$ .

From Fig. 15, we can see that at  $\sigma = 0.0$ , the neuron produces spike trains at regular intervals. However, as  $\sigma$  increases, i.e., as we add noise to the model, the neuron's spike train production becomes increasingly irregular, and more like the behavior we observed in the somatosensory neuron (see Fig. 5 and Fig. 7).

#### 4.1.4 Time varying current

Thus far, we have modeled the behavior of the integrate and fire neuron with respect to a constant injected current. However, in reality, different stimuli, as well as other brain processes, modulate the amount of current received by the neuron. Thus, the current injected into a neuron varies with time. We can model this by adding a time-varying component to the injected current. Figure 16. shows the behavior of the neuron when the injected current is a random walk. The equation describing this random walk is:

$$C_{t+1} = C_t + \Delta C_t \quad (8)$$

where  $\Delta C_t$  is defined:

$$\begin{cases} -1 & \text{if } R_t < 0.5 \text{ and } C_t > 0, \\ 1 & \text{if } R_t > 0.5 \text{ and } C_t < 2I, \\ 0 & \text{otherwise.} \end{cases}$$

And  $R_t$  is a random number between 0 and 1

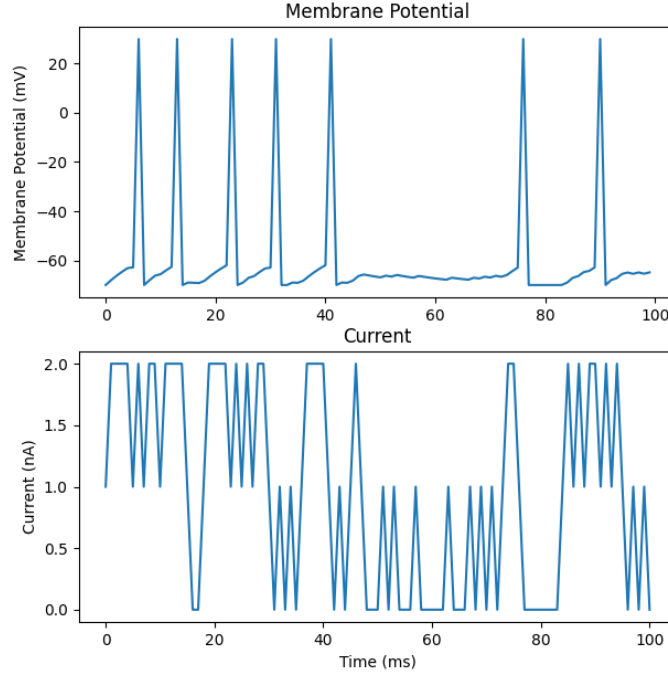


Figure 16: Noisy integrate and fire neuron activity over time when the injected current is a random walk.  $I_0 = 1$ ,  $\sigma = 0.001$ ,  $V_0 = -70mV$ ,  $\Delta t = 1ms$

As we can see from Fig. 16, as we vary the injected current, we also vary its spiking behavior. When there are periods of low current, the neuron fails to reach the threshold potential, and thus we do not see any spikes (eg. between 50ms and 75ms). This type of behavior is closer to what we would expect from a real neuron, which is always receiving varying input from other neurons, and thus a fluctuating current. x

## 4.2 The Hodgkin-Huxley model

While the integrate and fire model offers a good first approximation of the workings of individual neurons, it is not without its limitations. Foremost of which is the lack of an innate spiking mechanism. Recall, to produce a spike, we introduced a brute threshold into our model, and a brute maximum potential. Moreover, it collapsed the influence of all the different ions interacting with the cell into a single term,  $E_L$ . A better model of the neuron would have spike production as an emergent property, and account for the differences in ions, better reflecting the biological reality of neurons. The Hodgkin-Huxley (H & H) model is such a model.

#### 4.2.1 Voltage gated ion channels

Central to the H & H model is the idea of the voltage gated ion channels. From experimental results, H & H found that the cell membrane contains different types of voltage-gated ion channels, that regulate the flow of ions in and out of the cell. They are 'voltage-gated' because they open and close in response to changes in the membrane potential. Specifically, H & H identified the Potassium ( $K^+$ ) and Sodium ( $Na^+$ ) channels as the most important to the generation of action potentials.

The  $NA^+$  channels control flow of Sodium ions into the cell. They are therefore responsible for the initiation of the action potential when they open and allow large amounts of  $NA^+$  to rush into the cell and depolarize it. From their experiments, H & H found that  $NA^+$  channels contain 3 subunits which are responsible for opening and closing the channel. Represented in the model as  $m^3$ , these subunits open and close probabilistically based on the membrane potential.  $m^3$  represents the probability that the channel is open. The opening rate of the channel,  $\alpha_m$ , and the closing rate of the channel  $\beta_m$ , are given by the following equations, where  $V$  is the membrane potential:

$$\alpha_m = \frac{0.1(V + 40)}{1 - \exp[-0.1(V + 40)]} \quad \beta_m = 4 \exp[-0.0556(V + 65)] \quad (9)$$

The  $NA^+$  channels also contain an inactivation gate,  $h$ , which is responsible for inactivating the channel so that the neuron cannot depolarize indefinitely.  $h$  represents the probability that the channel is *not* inactive. The opening and closing rate of the inactivation gate is given by:

$$\alpha_h = 0.07 \exp[-0.05(V + 65)] \quad \beta_h = \frac{1}{1 + \exp[-0.1(V + 35)]} \quad (10)$$

The H & H model also accounts for the reversal potential of the  $NA^+$  channels,  $E_{NA}$ , which is the potential at which the flow of  $NA^+$  ions into the cell is equal to the flow of  $NA^+$  ions out of the cell. Moreover,  $\bar{g}_{NA}$  is the maximum specific conductance for  $NA^+$  channels.

The  $K^+$  channels control the flow of  $K^+$  ions in and out of the cell. They are responsible for the repolarization of the cell after the action potential. During the action potential, they slowly open to release  $K^+$  from the cell to return it to equilibrium. However, they close slowly, so they end up hyperpolarizing the cell, bringing the Membrane Potential below resting. The  $K^+$  channels contain 4 subunits, represented as  $n^4$ .  $n^4$  represents the probability that the channel is open. The opening and closing rates of the  $K^+$  channels are given by the following equations:

$$\alpha_n = \frac{0.01(V + 55)}{1 - \exp[-0.1(V + 55)]} \quad \beta_n = 0.125 \exp[-0.0125(V + 65)] \quad (11)$$

Likewise, the H & H model accounts for the reversal potential of the  $K^+$  channels,  $E_K$ . Moreover,  $\bar{g}_K$  is the maximum specific conductance for  $K^+$  channels.

The dynamics of these channels over time, are described by the following equation:

$$\frac{dx}{dt} = \alpha(V)(1 - x) - \beta(V)x \quad (12)$$

Finally, the H & H model accounts for the leak potential of the cell,  $E_L$ , which is the potential at which the flow of ions into the cell is equal to the flow of ions out of the cell. Moreover,  $\bar{g}_L$  is the maximum specific conductance for the leak channels.

Combining these equations, we get the full H & H model, where  $I$  is the injected current, and  $C$  is the membrane capacitance:

$$C \frac{dV}{dt} = \bar{g}_L(E_L - V) + \bar{g}_K n^4(E_K - V) + \bar{g}_{Na} m^3 h(E_{Na} - V) + I \quad (13)$$

#### 4.2.2 Simulating the H & H model

Like the integrate and fire model, we can solve the H & H model numerically using Euler's method. Figure 17 shows the behavior of the H & H neuron, as well as the gating variables, over 1000ms, given the following initial conditions:

$C = 1$ ,  $E_L = -54.5mV$ ,  $E_{Na} = 50mV$ ,  $E_K = -77mV$ ,  $\bar{g}_L = 0.3mS$ ,  $\bar{g}_{Na} = 120mS$ ,  $\bar{g}_K = 36mS$ ,  $V_0 = -54.4mV$ ,  $m_0 = 0.168$ ,  $h_0 = 0.247$ ,  $n_0 = 0.485$ ,  $\Delta t = 0.05ms$ , and  $I = 10nA$ .

Where  $m_0$ ,  $h_0$ , and  $n_0$  are the initial values of the gating variables given by:

$$x_0 = \frac{\alpha_x}{\alpha_x + \beta_x} \quad (14)$$

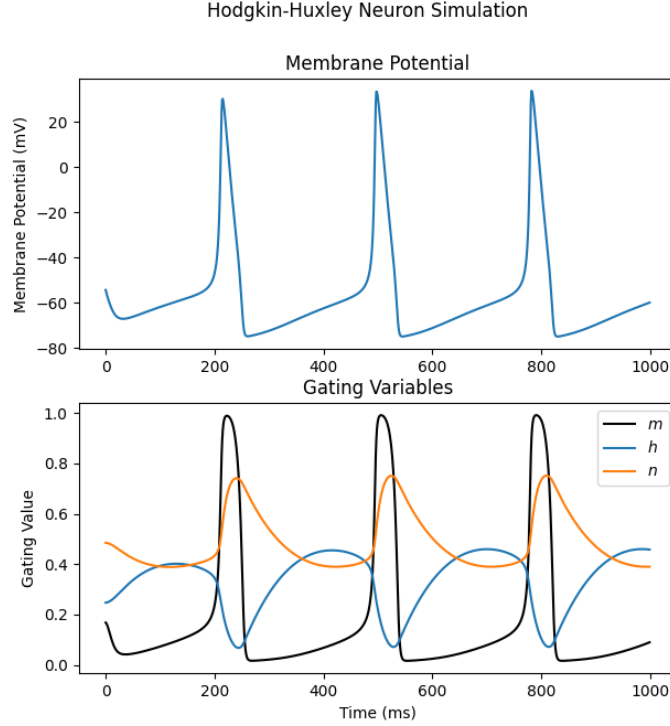


Figure 17: H & H model of a neuron, with an injected current of  $I = 10nA$ .

From Fig. 17, we see that the model generates the kind of spiking behavior we would expect from a real neuron, without imposing a manual threshold. Rather, the spiking is produced by the interplay of the gating variables,  $m$ ,  $h$ , and  $n$ , and the membrane potential  $V$  over time.

Initially,  $V$  decreases. However, as  $V$  fluctuates, both  $m$  and  $h$  increase, while  $n$  decreases. This leads to a net increase in  $V$ , which in turn increases  $n$ , leading to a positive feedback loop in which the  $n$ , and thus  $V$ , increases exponentially (around 196ms). The  $V$  that this behavior occurs at in our model is around  $-50mV$ . This is referred to as the spiking threshold. This dynamic captures the rapid depolarization of the cell that occurs when the  $NA^+$  channels open.

As the spike occurs,  $h$  decreases rapidly, which represents the inactivation the  $NA^+$  channels. Moreover, the probability that the  $K^+$  channels are open,  $n$ , increases. As noted above, biologically this process is much slower, a fact which is reflected in the more gradual initial slope of  $n$  compared to  $m$ . Since  $\bar{g}_{NA}m^3h(E_{NA} - V)$  approaches 0 for small values of  $h$ , and  $E_L$  and  $E_K$  are both negative, we get a massive downward pressure on  $V$ . This is dynamic occurring right after the exponential increase in  $V$  and is what creates the 'spike' in  $V$ .

Again, the  $K^+$  channels are slow to close. This is reflected in the gradual decrease in  $n$  after the spike. This gradual decrease causes the net change in  $V$  to be negative for a long time, leading to values of  $V$  below the resting potential. As  $V$  decreases,  $m$  and  $h$  begin to increase again, putting upwards pressure on  $V$ . This corresponds to the de-inactivation channels, and subsequent opening, of the  $NA^+$  channels after a spike in a real neuron. Thus, the cycle repeats and the neuron spikes again.

### 4.2.3 H & H model with varying injected current

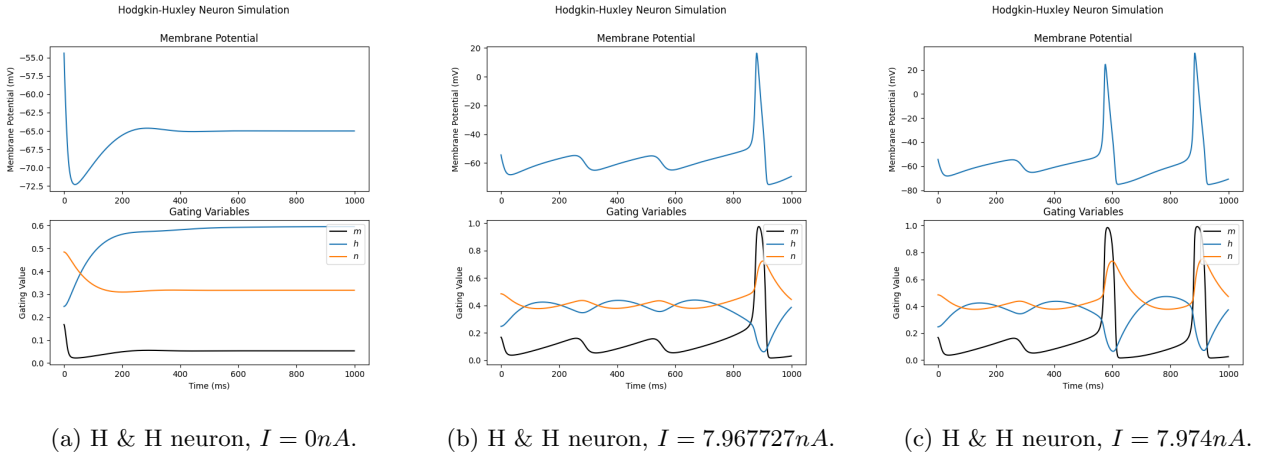


Figure 18: H & H model of a neuron, with varying injected currents.

Figure 18 shows the behavior of the H & H neuron with the same initial conditions as before, but with various levels of injected current. As we can see from the figure, the neuron spikes only when the injected current,  $I$  is above a certain level. When  $I = 0$ , the resultant voltage is not large enough to open the  $Na^+$  channels. Thus,  $m$  never increases enough to begin the positive feedback loop. Therefore, no action potential occurs. Given our initial conditions, the amount of current needed to start this process is around  $7.967nA$ . At this level of current, the fluctuation in voltage is such that enough  $Na^+$  channels open to begin the positive feedback loop (around 850ms). The neuron starts spiking repeatedly when the current is at or above  $7.974nA$ .

Thus, the H & H model is able to capture the behavior of neurons in response to varying stimuli, without the need for a manual threshold. Rather, the spiking behavior is an emergent property of the model, arising from the dynamics of the gating variables and the membrane potential over time. It therefore provides a more accurate model compared to the integrate and fire model.

### 4.2.4 Summary

In this section, we have explored the dynamics of individual neurons. We began with the simple integrate and fire model, which captured the basic properties of the neuron as a circuit, but lacked an innate spiking mechanism, among other biological factors. We then examined the H & H model of the neuron, which accounted for the affect of different ions on the cell, mediated by the voltage gated ion channels. Moreover, this model is able to innately produce the spiking behavior found in real neurons, without the need for a manual threshold.

## 5 Conclusion

In this report, we have explored the dynamics of the neuron at two different levels. Firstly, at the level of its macro dynamics, in terms of spike trains. We saw that neurons are probabilistic and noisy, and that their response to a stimulus is in part mediated by the intensity of the stimulus. Secondly, we explored the dynamics of the neuron at the micro level, in terms of how it generates spikes. We saw two models: Integrate and Fire, and Hodgkin and Huxley. While integrate and fire captured the circuit-like dynamics of neurons, it was biologically implausible. The H & H model builds on the foundation of the integrate and fire model, but adds the biological complexity of the neuron, and is able to innately generate the spiking behavior. It is thus a much better model of the neuron.

However, the brain contains more than a single neuron, and they do not act alone. Thus, while we have simulated and analyzed the behavior of a single neuron, we have missed the interactions between neurons. Thus, our analysis is limited with respect to the brain as a whole. In order to analyze the brain as a whole, we will need to look at networks of neurons.